SOFT PROTON FLUXES IN AND AROUND EARTH'S DISTANT MAGNETOTAIL

Dušan Budjáš, Petteri Nieminen, Piers Jiggens, Giovanni Santin, Eamonn Daly

European Space Agency, Space Environment and Effects Section, ESTEC, Noordwijk 2200AG, The Netherlands, Email: Dusan.Budjas@esa.int

ABSTRACT

The second L-class (large) mission in ESA's Cosmic Vision programme will be an X-ray telescope named Athena, planned to operate at the L2 Lagrange point of the Sun-Earth system. Current large X-ray space telescopes XMM-Newton and Chandra have encountered unexpectedly high background and degradation in their detectors from protons in energy ranges between 10 keV and 1 MeV (called "soft protons" hereafter). This is an important issue for Athena, as no X-ray telescope has been deployed at L2 so far and the soft proton environment there is poorly known. We present an analysis of long-term measurements of soft proton fluxes by several spacecraft including Geotail, Artemis and ACE in space around Earth from L1 to L2. The ultimate goal of this work is to provide the best possible picture of soft proton fluxes and of their origin (solar or magnetospheric).

1. INTRODUCTION

Athena is an ambitious observatory envisioned to provide high resolution X-ray imaging, timing and spectroscopy capabilities that are far beyond those of any existing facilities [1]. Athena is designed to address key open topics in modern astrophysics, from physical conditions in hot plasmas in a wide range of astrophysical environments, through the physics of accretion, super-massive black hole growth and galaxy evolution, to cosmologically relevant properties of hot baryons in galaxy clusters. In particular, desired observations of warm and hot intergalactic plasma, galaxy cluster outskirts and distant active galactic nuclei drive requirement of low background.

Current large X-ray space telescopes XMM-Newton and Chandra have encountered in their detectors high background as well as radiation damage from protons in energy ranges between 10 keV and 1 MeV [2, 3]. These "soft protons" are funnelled through the focusing Wolter-I type grazing incidence optics of X-ray observatories more efficiently than was initially expected. Later Monte Carlo simulations [4, 5] showed that this process can explain the high background. The flux is known to be extremely variable, with sharp increases occurring over time scales as short as minutes – sometimes referred to as "soft proton flares" [6, 7].

Possible sources of soft protons include interplanetary coronal mass ejections and their associated shocks, flaring near open coronal field lines resulting from coronal holes and acceleration events in Earth's magnetosphere. Inside Earth's magnetotail, which extends in the direction of and beyond the L2 point, the region with typically the highest fluxes of soft protons is the plasma sheet [8]. The tail is a highly dynamic structure and plasma sheet encounters with spacecraft at L2 are likely [9].

No X-ray telescope has been deployed at L2 so far and the soft proton environment there is poorly known. In particular their flux and spatial distribution around this region are not well characterised on long timescales relevant for the duration of space missions. Furthermore, solar particle fluence models, such as e.g. the Emission of Solar Protons (ESP) model [10], consider only solar particle events (SPEs) with fluences above a certain threshold, and quiet-time fluxes or flare events below threshold are not taken into account. Athena scientific requirements [11] specify a limit on background caused by particles entering the optics for > 90% of observing time. Depending on the phase of the solar cycle SPEs could fall into the worst 10% of observing time and particle flux not considered in SPE-based models could instead dominate the background rate.

The aim of this study is to use data from spacecraft that have measured particle fluxes in the soft proton energy range in the relevant regions of space to characterise this component of space environment, focusing on fluxes occurring outside SPEs.

2. MEASUREMENTS BY SPACE PROBES

The environment of the Earth's distant magnetotail was surveyed in 1992-1994 by the NASA/ISAS Geotail spacecraft, and in 2009-2011 by the twin NASA Artemis probes. Additionally, soft proton flux measurements outside of Earth's magnetosphere are performed by a number of spacecraft positioned around the L1 point on the Sun-ward side of Earth, including ACE, Wind, and SOHO, starting from 1996.

In this work we use data obtained by Geotail in 1994, and by Artemis P1, Artemis P2 and ACE in 2010-2011. The ACE EPAM data were downloaded from [12], the rest from NASA's Coordinated Data Analysis Web [13]. We use undifferentiated ion fluxes in this study, with the exception of the ACE ULEIS data, from which we use the proton channel.

Overview of the instruments is given in Tab. 1. More detailed description can be found in the references listed in the table. Geotail orbit during the studied period is depicted in Fig. 1, spending most of the time in distant magnetotail or magnetosheath. The Artemis probes were orbiting around the Lagrange points of the Earth-Moon system, i.e. at a roughly similar orbit as the Moon, periodically spending about ¼ of the time in magnetotail or magnetosheath and about ¾ of the time in the solar wind. ACE orbits around the Sun-Earth L1 point, always in an environment dominated by the solar wind.

Table 1. Instrument descriptions.

Instrument	Energy range [keV]	Description
Geotail EPIC/ICS [14]	60 – 1350	Solid state telescopes, covering ~37° above and below ecliptic
Artemis P1 & P2 SST [15]	30 – 6000	Solid state telescopes, covering almost 4π sr
ACE EPAM LEMS120 [16]	47 – 4750	Low Energy Magnetic Spectrometer, covering ±30° around 120° direction from the Sun
ACE ULEIS [17]	160 – 7200 (p^+ channel)	Ultra-Low Energy Isotope Spectrometer pointing 60° from the Sun direction

3. DATA ANALYSIS

First, non-physical data points were removed from the data sets. The ICS instrument on Geotail applies filters of various thicknesses to protect the detectors from increased particle fluxes. This shifts to higher values the energy ranges which the detector channels are sensitive to, therefore the data are interpolated to maintain consistent energy bins. The SST instruments on Artemis probes gradually change energy calibration over time, but this was considered negligible (< 3 keV over the studied period). Geotail and Artemis data were provided with mean energy values per bin. ACE data only contain the edge values of the bins; the geometric mean was used to approximate the mean energy value per bin.

Fig. 2 shows the Geotail flux data over a period of 24 hours in the original cadence of about 100 s. The flux variability is high on this timescale, as is observed also in soft proton flares e.g. in XMM-Newton background [6, 7]. Nevertheless, to facilitate the characterisation of the fluxes over long periods on the time scales of spacecraft lifetimes, in the next step the data were averaged into one-day intervals.

In Fig. 3, daily average fluxes from three Geotail EPIC/ICS channels are plotted over the studied period from January to November 1994. Colour-coded bands represent approximate location of the probe in different

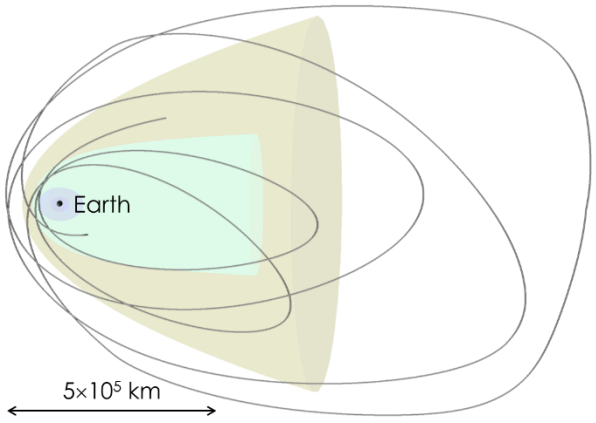

Figure 1. Geotail trajectory in the Geocentric Solar Ecliptic coordinates during the studied period in 1994 visualised with 3DView [18]. The Sun is to the left and the view is from above the ecliptic plane. A static representation of bow shock (yellow), magnetopause (green) and the large radiation belt (blue) is shown.

magnetospheric regions, determined using the visualisation of Geotail orbit and of static bow shock and magnetopause model in the software 3DView [18] as shown in Fig. 1, as well as days affected by SPEs taken from the reference event list of the SEPEM tool [19].

Fig. 4 shows the daily average fluxes from two energy channels from the SST instruments on Artemis P1 and P2 probes. The time frame chosen for analysis occurs after both probes entered orbits around the Earth-Moon Lagrange points and before their transfer to lunar orbits. In this period both probes nearly simultaneously encounter similar magnetospheric environment. Artemis data contain a flag identifying whether the spacecraft is encountering solar wind or not (i.e. it is located within Earth's magnetosheath/magnetotail). The solar wind flag of each spacecraft is indicated as colour-coded bands, as well as the SPE days. The periodicity of the spacecraft location, given by their orbits, is apparent. The solar wind flag was cross-checked with the orbit visualisation software and some inaccuracies were corrected.

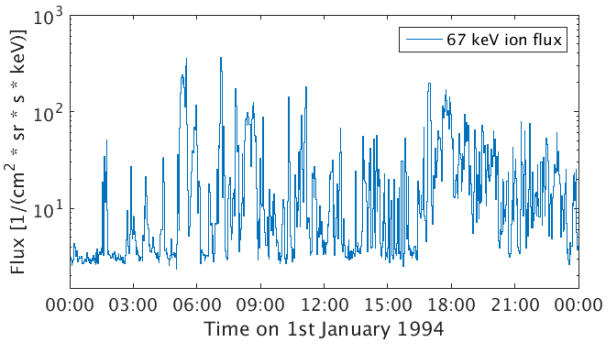

Figure 2. Geotail EPIC/ICS ion flux variation over a period of 24 hours on 1st January 1994.

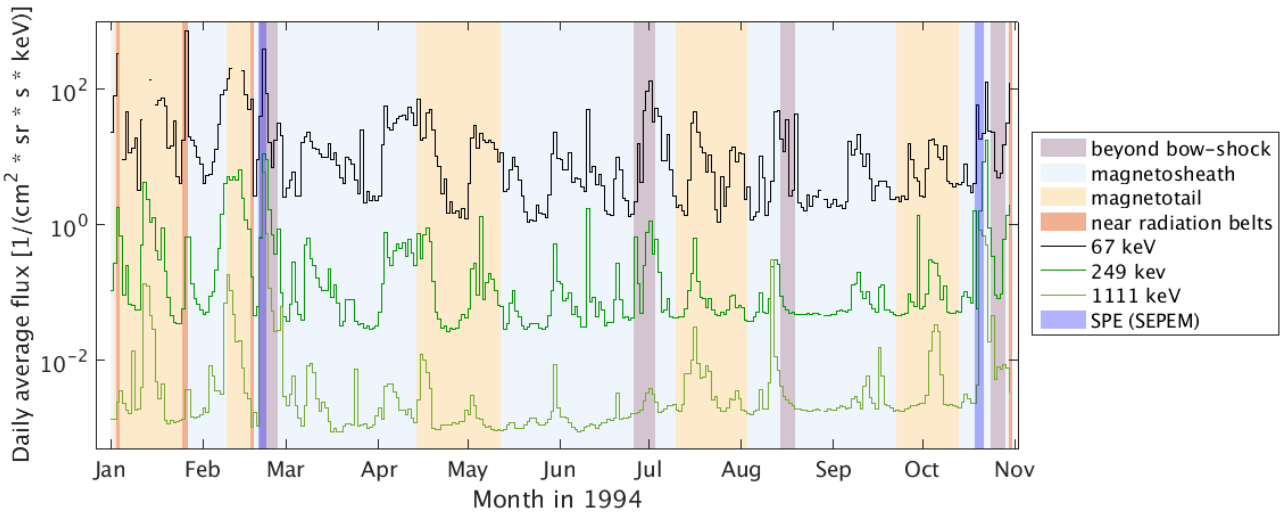

Figure 3. Time variation of Geotail EPIC/ICS daily average ion fluxes in three energy channels over the studied period.

In a final step, average spectra were obtained for the studied periods. These are shown in Fig. 5 comparing Artemis and Geotail spectra, and in Fig. 6 comparing Artemis and ACE spectra. The days affected by SPEs and, for Geotail also passages close to radiation belts, were excluded from the average, and the Artemis data were split into separate spectra averaged over the periods spent in the solar wind and in the magnetosheath/magnetotail. Energy bins lower than 99 keV are not shown in the Geotail spectrum, because the filters applied to the ICS instrument when high flux levels are encountered make it selectively insensitive to lower energy particles (this is also apparent in Fig. 3 with the 67 keV channel featuring more gaps in the data than the higher energy channels). In Fig. 5 the Artemis spectra are shown separately for each of the two probes, demonstrating that they are consistent with each other. In Fig. 6 these two datasets were combined into a single spectrum.

4. DISCUSSION

The Artemis data inside the magnetosheath and magnetotail show an increase of flux and a steeper slope of the spectrum below ~100 keV compared to the outside of Earth's magnetosphere. The Artemis fluxes outside the magnetosphere are for the most part compatible with the ACE EPAM measurements. On the other hand the ACE ULEIS spectrum shows slightly higher flux than both EPAM and Artemis despite that only the proton flux is shown for ULEIS and both the EPAM and Artemis data include also helium and other species. This could be perhaps related to the different look directions of the instruments, with ULEIS pointing more close to the direction of the Sun. The flux measured by Geotail is clearly higher than the other data, especially at lower energies. At least part of the difference could be related to long term variability of the fluxes, as the Geotail data were taken in a

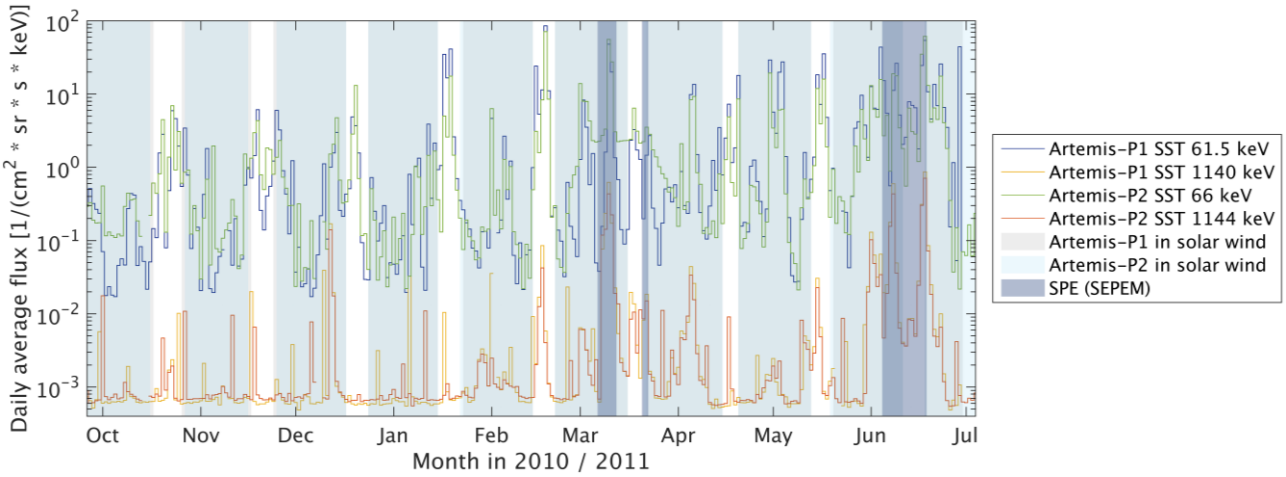

Figure 4. Time variation of Artemis SST daily average ion fluxes in three energy channels over the studied period.

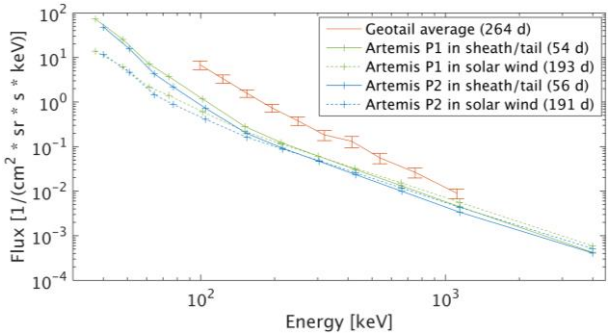

Figure 5. Geotail EPIC/ICS average ion spectrum compared to Artemis P1 and P2 spectra averaged over periods in solar wind and mangetosheath/magnetotail.

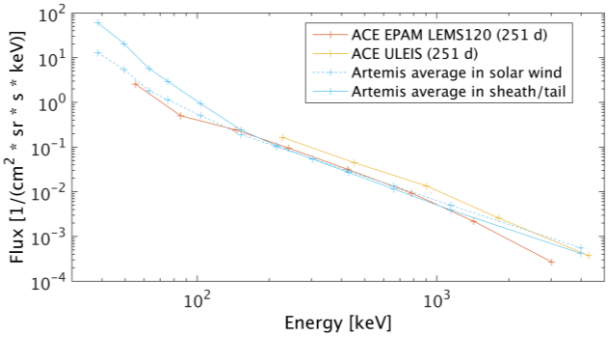

Figure 6. ACE EPAM/LEMS 120 and ULEIS average spectra compared to combined Artemis average ion spectra in solar wind and mangetosheath/magnetotail.

different phase of a different solar cycle than the ACE and Artemis data. Finally, visual examination of Fig. 3 doesn't indicate any obvious correlation of the Geotail ICS fluxes with presence in magnetotail or magnetosheath.

The presented analysis is part of an ongoing work to characterise the soft proton environment that will be encountered by the Athena X-ray telescope. The analysis will be further extended with improved magnetospheric region identification, and comparison with additional data from these and other instruments/spacecraft.

Furthermore, the periods covered in this analysis occurred during relatively quiet parts of the solar cycle and we have excluded SPE contributions to the average flux. In the covered periods these contributions manifest themselves only at the high-energy end of the spectra, but they would likely be much higher in the whole energy range during peaks of solar activity, thus it is another important topic for further study.

Although the results presented here are only the beginning of a comprehensive characterisation of the soft proton environment, they can be used to obtain a crude estimate of average background caused by soft protons in the Athena detectors in relatively quiet periods of solar cycle. In order to do this, we have used a Geant4 [20] based tool GRAS [21] to simulate proton transfer through the different materials and into the Athena detectors. Thicknesses and composition of the various material layers were obtained from [22, 23]. The efficiency of transfer of the initial omnidirectional proton flux through Athena-like silicon-pore optics into the focal plane was previously estimated using GRAS simulation [24, 25] and ray tracing [26], both employing an approximation of Firsov scattering process. Both studies obtained a value of the proton transfer efficiency of around $3 \cdot 10^{-5}$ which we apply in our calculation. The output from our GRAS simulation, performed with a flat source proton energy distribution is then convolved with a power law fit to the Artemis spectra (Fig. 6) in the applicable energy range (< 100 keV). Possible energy losses in the transfer through the silicon-pore optics are neglected. Figs. 7 and 8 show the resulting background spectra in the X-IFU and WFI instruments, respectively in the solar wind and magnetosheath/magnetotail environments. WFI is simulated with and without an additional optical filter mentioned in [22, 23]. Dotted lines in the plots depict the scientific requirements on the soft proton background in

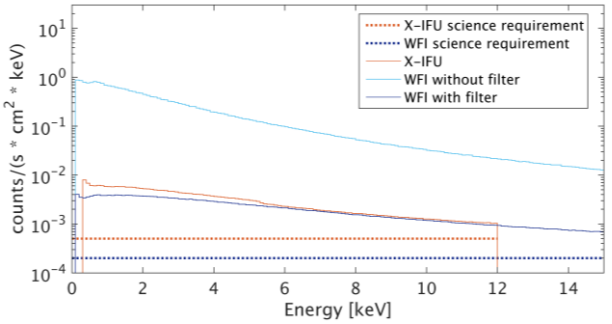

Figure 7. Simulated background spectra in the Athena instruments as described in text, based on Artemis proton fluxes in solar wind environment.

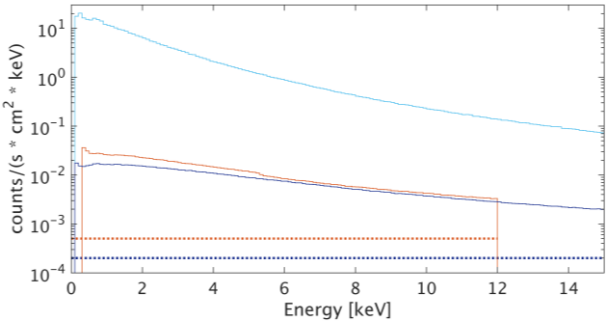

Figure 8. Simulated background spectra in the Athena instruments based on Artemis proton fluxes in magnetosheath/magnetotail environment. See Fig. 7 for legend.

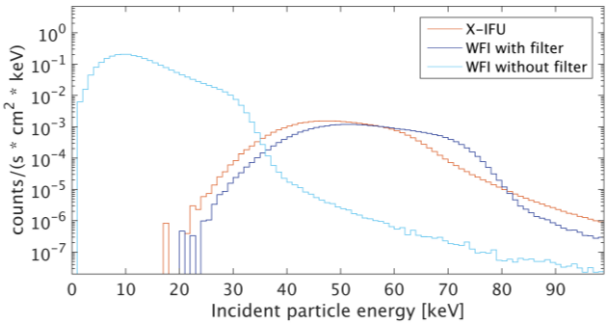

Figure 9. Simulated distribution of initial energies of protons generating background in Athena instruments, in solar wind environment.

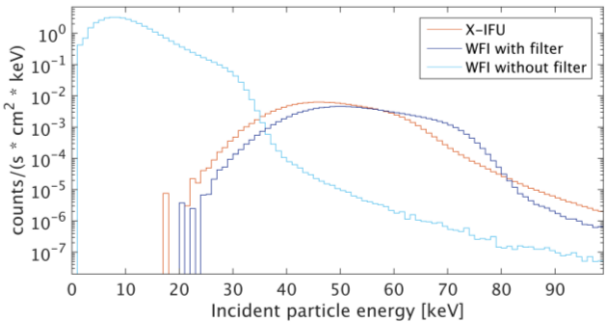

Figure 10. Simulated distribution of initial energies of protons generating background in Athena instruments, in magnetosheath/magnetotail environment.

Athena as defined in [11]. Figs. 9 and 10 show the corresponding distributions of initial energies of the protons that generate background in the detectors.

The largest uncertainty in the simplified background estimate presented above likely concerns the proton transfer efficiency through the silicon-pore optics. The physics of grazing-angle proton scattering is poorly known and experiments with protons beams are necessary before more accurate predictions can be made. In the case of WFI without the additional filter, the source proton spectrum had to be extrapolated down to a few keV, contributing further significant uncertainty. Another large uncertainty concerns the long term variability of the soft proton fluxes as indicated by the difference of Geotail and Artemis data in Fig. 5 (Geotail data could not be used in the background estimation as they do not extend low enough in energy). If the assumptions used here are in the right order of magnitude, it is clear that additional reduction of the proton flux will be necessary for Athena. A magnetic diverter is being studied for this purpose. Efficient deflection will be necessary for up to ~80 keV protons. While the case of WFI without filer results in a background rates more than two orders of magnitude higher than the results for XIFU and WFI with filter, the proton energies responsible are mostly below ~40 keV, which would be comparatively easier to magnetically deflect.

5. AKNOWLEDGEMENTS

We acknowledge NASA contract NAS5-02099 and V. Angelopoulos for use of data from the THEMIS Mission. Specifically: D. Larson and R. P. Lin for use of SST data. We also acknowledge T. Lui for use of EPIC data from the GEOTAIL mission, and E. C. Stone, R. Gold, G. Mason and G. Ho for the use of EPAM and ULEIS data from the ACE mission.

6. REFERENCES

1. Barcons, X. et al. (2015). Athena: the X-ray observatory to study the hot and energetic Universe. J. Phys: Conf. Series 610, 012008.
2. Turner, M.J.L. et al. (2001). The European Photon Imaging Camera on XMM-Newton: The MOS cameras. A&A 365, L27-L35.
3. Katayama, H. et al. (2004). Properties of the background of EPIC-pn onboard XMM-Newton. A&A 414, 767-776.
4. Nartallo, R. et al. (2001). Low-Angle Scattering of Protons on the XMM-Newton Optics and Effects on the On-Board CCD Detectors. IEEE TNS 48, 1815-1821.
5. Lei, F. et al. (2005). Update on the use of Geant4 for the simulation of low-energy protons scattering off X-ray mirrors at grazing incidence angles. IEEE TNS 51, 3408-3412.
6. De Luca, A. and Molendi, S. (2004). The 2–8 keV cosmic X-ray background spectrum as observed with XMM-Newton. A&A 419, 837-848.
7. Pradas, J. and Kerp, J. (2005). XMM-Newton data processing for faint diffuse emission. A&A 443, 721-733.
8. Sarafopoulos, D.V. et al. (1997). Spatial structure of the plasma sheet boundary layer at distances greater than 180 RE as derived from energetic particle measurements on GEOTAIL. Ann. Geo. 15, 1246-1256.
9. Christon, S.P. et al. (1998). Magnetospheric plasma regimes identified using Geotail measurements 2. Statistics, spatial distribution, and geomagnetic dependence. J. Geophys. Res. 103, 23521-23542.
10. Xapsos et al. (1999). Space Environment Effects: Model forEmission of Solar Protons (ESP) –Cumulative and Worst-Case Event Fluences. NASA/TP-1999-209763.
11. Athena Science Requirements Document. Date 18/01/2016. SRE-S/ATH/2015/01.
12. http://www.srl.caltech.edu/ACE/ASC/level2/lvl2DATA_EPAM.html

13. http://cdaweb.gsfc.nasa.gov/
14. Williams, D.J. et al. (1994). Geotail Energetic Particles and Ion Composition Instrument. J. Geomag. Geoelectr., 46, 39-57.
15. Angelopoulos, V. (2008). The THEMIS mission. Space Sci. Rev. 141, 5-34.
16. Gold, R.E. et al. (1998). Electron, Proton and Alpha Monitor on the Advanced Composition Explorer Spacecraft. Space Sci. Rev. 86, 541-562.
17. Mason, G.M. et al. (1998). The Ultra-Low Energy Isotope Spectrometer (ULEIS) for the ACE spacecraft. Space Sci. Rev. 86, 409-448.
18. http://3dview.cdpp.eu/
19. http://dev.sepem.oma.be/
20. Agostinelli, S. et al. [GEANT4 Collaboration] (2003). Geant4: a simulation toolkit. Nucl. Instrum. Meth. A506, 250.
21. Santin, G., Ivanchenko, V., Evans, H., Nieminen, P., Daly, E. (2005). GRAS: A general-purpose 3-D modular simulation tool for space environment effects analysis. IEEE TNS 52, 2294 -2299.
22. ATHENA CDF Study Report: CDF-150(A), November 2014.
23. ATHENA Assessment Study Report. December 2011. ESA/SRE(2011)17
24. Santin, G., Rodgers, D.J., Fioretti, V. (2009). Impact of Space Protons and Electrons Scattering through the IXO Telescope Mirrors. IEEE NSS Conference Record, 459-461.
25. ATHENA Environmental Specification. Date 08/07/2014. TEC-EES/2014.89/DR
26. Perinati, E. et al. (2010). Estimate of the background for the X-Ray Microcalorimeter Spectrometer onboard of IXO. Proc. of SPIE 77323X, 1-8.